Neurobiology of Disease 44 (2011) 284–291

Contents lists available at ScienceDirect

Neurobiology of Disease

journal homepage: www.elsevier.com/locate/ynbdi

Synaptic dysfunction in hippocampus of transgenic mouse models of Alzheimer's disease: A multi-electrode array study

Seon-Ah Chong [a,b], Iryna Benilova [f,g], Hamdy Shaban [e], Bart De Strooper [f,g], Herman Devijver [d], Dieder Moechars [e], Wolfgang Eberle [a], Carmen Bartic [a,c], Fred Van Leuven [d,*], Geert Callewaert [b,**]

[a] Bio-Electronic Systems, Imec, Kapeldreef 75, Leuven, Belgium
[b] Research Group Neurodegeneration, KULeuven, Kortrijk, Belgium
[c] Laboratory of Solid State Physics and Magnetism, Department of Physics and Astronomy, KULeuven, Leuven, Belgium
[d] Experimental Genetics Group - LEGTEGG, KULeuven, Leuven, Belgium
[e] CNS discovery, Janssen, Turnhoutseweg 30, Beerse, Belgium
[f] Department for Molecular and Developmental Genetics, Flanders Institute for Biotechnology (VIB), Leuven, Belgium
[g] Laboratory for the Research of Neurodegenerative diseases, Center for Human Genetics, KULeuven, Leuven, Belgium

ARTICLE INFO

Article history:
Received 15 February 2011
Revised 19 May 2011
Accepted 6 July 2011
Available online 18 July 2011

Keywords:
AD transgenic mice
Amyloid
Tau
Synaptic dysfunction
Hippocampal slices
Multi-electrode arrays
Dual recordings

ABSTRACT

APP.V717I and Tau.P301L transgenic mice develop Alzheimer's disease pathology comprising important aspects of human disease including increased levels of amyloid peptides, cognitive and motor impairment, amyloid plaques and neurofibrillary tangles. The combined model, APP.V717I×Tau.P301L bigenic mice (biAT mice) exhibit aggravated amyloid and tau pathology with severe cognitive and behavioral defects. In the present study, we investigated early changes in synaptic function in the CA1 and CA3 regions of acute hippocampal slices of young APP.V717I, Tau.P301L and biAT transgenic animals. We have used planar multi-electrode arrays (MEA) and improved methods for simultaneous multi-site recordings from two hippocampal sub-regions. In the CA1 region, long-term potentiation (LTP) was severely impaired in all transgenic animals when compared with age-matched wild-type controls, while basal synaptic transmission and paired-pulse facilitation were minimally affected. In the CA3 region, LTP was normal in Tau.P301L and APP.V717I but clearly impaired in biAT mice. Surprisingly, frequency facilitation in CA3 was significantly enhanced in Tau.P301L mice, while not affected in APP.V717I mice and depressed in biAT mice. The findings demonstrate important synaptic changes that differ considerably in the hippocampal sub-regions already at young age, well before the typical amyloid or tau pathology is evident.

Introduction

Transgenic mouse models overexpressing human mutant amyloid precursor protein (APP) or microtubule associated protein tau show various pathological hallmarks of Alzheimer's disease (AD) (Denk and Wade-Martins, 2009; Goetz and Ittner, 2008; Jaworski et al., 2010). Bigenic or triple transgenic mice have also been developed to study the complexity of AD by the combined amyloid and tau pathology (Lewis et al., 2001; Oddo et al., 2003). Here, we investigated early synaptic changes of young adult (4–6 months) tau and APP transgenic mice, separately and combined in a bigenic model that recapitulates amyloid and tau pathology synergistically (Terwel et al., 2008). APP.V717I transgenic mice progressively develop increased levels of APP intermediates and soluble amyloid peptides (Aβ) by 3 months of age, causing early cognitive impairment before clear deposition of extracellular plaques after 12 months (Moechars et al., 1999). Similarly, age-dependent tau hyperphosphorylation is developed in Tau.P301L transgenic mice by 3 months of age, leading to neurofibrillary tangles (NFT) and motor deficits at older age (Boekhoorn et al., 2006; Dutschmann et al., 2010; Terwel et al., 2005). APP.V717I×Tau.P301L bigenic (biAT) mice develop combined amyloid plaques and NFT from 10 months, however amyloid accumulation is already observed at young age (3 months) (Terwel et al., 2008).

Tau and APP transgenic models show altered synaptic transmission and plasticity in the hippocampus (Fitzjohn et al., 2001; Rosenmann et al., 2008). Synaptic alterations have been observed at young age, well before amyloid deposits or tau aggregates are evident. Different APP transgenic strains exhibit LTP deficits at 2–6 months of age either associated or not with changes in pre- and basal synaptic transmission in the CA1 region (Giacchino et al., 2000; Hsia et al., 1999; Larson et al., 1999; Moechars et al., 1999; Saganich et al., 2006). Synaptic dysfunctions in young tau transgenic models have not been studied extensively. A double tau mutant model did not show deficit in basal synaptic transmission in CA1 at 6 months of age (Schindowski

* Corresponding author. Fax: +32 16 345 871.
** Corresponding author. Fax: +32 56 246 994.
E-mail addresses: fred.vanleuven@med.kuleuven.be (F. Van Leuven), Geert.Callewaert@kuleuven-kortrijk.be (G. Callewaert).
Available online on ScienceDirect (www.sciencedirect.com).

0969-9961/$ – see front matter © 2011 Elsevier Inc. All rights reserved.
doi:10.1016/j.nbd.2011.07.006

et al., 2006) while LTP enhancement in the dentate gyrus was observed in 2-month-old single tau mutant mice (Boekhoorn et al., 2006). These early synaptic effects of amyloid or tau are thought to cause subtle cognitive changes and result in early mild cognitive impairment (MCI) before evident pathology is observed (Allegri et al., 2008).

On the other hand, studies of synaptic transmission and plasticity have been mainly limited to the CA1 region or the dentate gyrus (DG) of the hippocampus. Synaptic mechanisms, however, vary regionally in the hippocampus, and the mossy fiber-CA3 synapse displays some unusual and different forms of synaptic plasticity (Nicoll and Schmitz, 2005; Yeckel et al., 1999). Multi-electrode (or microelectrode) arrays (MEAs) offer an efficient *in vitro* test-platform allowing cell stimulation and extracellular recording at multi-sites simultaneously (Arnold et al., 2005; Hill et al., 2010; Li et al., 2007; Oka et al., 1999). We exploited the advantages of MEAs to develop a simple method to examine early synaptic effects of amyloid peptides and protein tau in young AD transgenic mouse models APP.V717I, Tau.P301L and APP.V717I×Tau.P301L bigenic mice. Synaptic transmission and plasticity was monitored simultaneously in the CA1 and CA3 regions of acutely prepared hippocampal slices, in order to compare age-matched APP.V717I, Tau.P301L and biAT transgenic mice to wild-type mice at young age, before onset of the typical AD-related pathology of amyloid plaques and NFT.

Material and methods

Transgenic mice

Synaptic transmission was analyzed in three transgenic mouse models, APP.V717I, Tau.P301L and APP.V717I×Tau.P301L bigenic (biAT) mice while wild-type (WT) mice were used as controls. Generation and phenotypic characterization of the transgenic mice was described previously (Moechars et al., 1999; Terwel et al., 2005, 2008). All mice analyzed were males of 4–6 months old, generated and maintained in the same FVB/N genetic background. Use of animals and procedures were approved by the Ethical Committee for Animal Welfare (ECD, Ethische Commissie Dierenwelzijn) of KULeuven and IMEC.

Acute hippocampal slice preparations

Mice were anesthetized with CO_2 and decapitated, and whole brains were quickly removed and placed in a vibratome chamber (Leica Microsystems, Germany), filled with ice-cold artificial cerebrospinal fluid (ACSF) solution containing (in mM) 125 NaCl, 2.5 KCl, 2 $CaCl_2$, 1 $MgCl_2$, 1.25 KH_2PO_4, 25 $NaHCO_3$, and 25 glucose, saturated with 95% O_2/5% CO_2 (pH 7.2–7.3 and 325 mOsm/kg). Hippocampi were horizontally cut at 250 µm trimmed of cortical tissue, cut between CA3 and CA1 by a surgical blade under a dissection microscope and allowed to recover in oxygenated ACSF solution at room temperature for at least 2 h. Hippocampal slices were transferred to a 200/30 MEA and continuously perfused with oxygenated ACSF (3 ml/min) at 31 °C.

Preparation of beta-amyloid oligomers

Aβ oligomers were prepared as described in Kuperstein et al. (2010). In brief, Aβ peptide was dissolved at a concentration of 1 mg/ml in hexafluoroisopropyl alcohol (HFIP, Aldrich, USA), and Aβ42 and Aβ40 were then mixed in molar ratio 3:7. HFIP was evaporated using a gentle stream of nitrogen gas and the peptide film was resolved using DMSO at a final concentration of 1 mg/ml. The peptide was separated from DMSO using a 5 ml HiTrapTM desalting column (GE Healthcare, Sweden) and eluted into 50 mM Tris and 1 mM EDTA buffer (pH 7.5). The peptide concentration was measured using the Bio-Rad Protein assay (Bio-Rad Laboratories GmbH, Germany). For slice treatment, Aβ was diluted in ACSF solution to a final concentration of 1 µM.

MEA recordings

Extracellular stimulation and recording were performed by Multi-Electrode Arrays (MEA 60 system, Multi Channel Systems, Germany). The system consists of a MEA 1060-BC pre-amplifier, a filter amplifier and four channel stimulus generator (STG 2004). MEAs for hippocampal slices have 8×8 (60) planar titanium nitride (TiN) electrodes with 30 µm diameter and 200 µm spacing. Slice position and contact with electrodes were ensured by slice grids (ALA Scientific Instruments, USA). Electrical stimulation and recording was performed simultaneously in the isolated region of CA1 and CA3 separated by transverse cut. In the CA1 region, stimulation electrodes were located under Schaffer collaterals, and evoked field excitatory postsynaptic potentials (fEPSPs) were monitored at proximal stratum radiatum and stratum pyramidale. CA3 fEPSPs were recorded at CA3 stratum radiatum by stimulating stratum lucidum. One electrode of the array was used as a reference electrode (for details see Fig. 1). Mossy fiber responses of CA3 were verified by frequency facilitation (FF) protocol (Nicoll and Schmitz, 2005) before recordings. Different electrodes under stratum lucidum were tested with increasing frequencies (0.05 to 2 Hz) until CA3 pyramidal cells show robust facilitation. Only electrodes showing FF were chosen for LTP stimulation and recording.

For LTP experiments, first input/output (I/O) curves were obtained in CA1 and CA3 and the stimulus intensity was adjusted to produce 40% fEPSP of its maximal response. Test stimuli were delivered every 60 s with biphasic voltage pulses for 200 µs. After recording of stable baseline for 30 min, LTP was induced by 2 trains of high frequency stimulation (HFS; 100 Hz) with 20 s interval. To ensure input specificity and viability of slices, a second electrode was selected in the CA1 subicular region to stimulate a second input independent from the tetanized input. Paired pulse facilitation (PPF) was measured

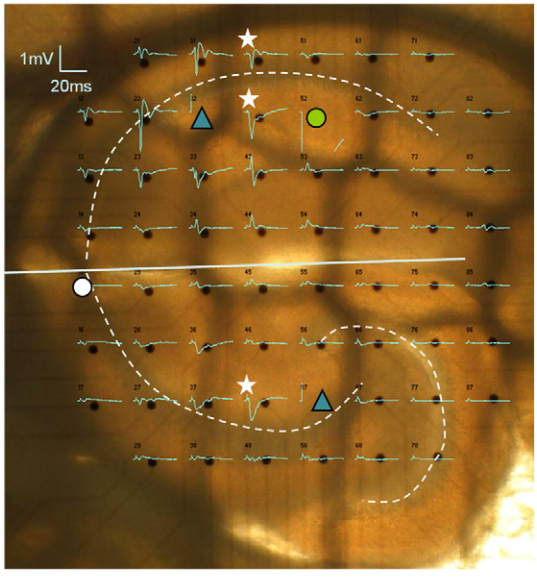

Fig. 1. Recording synaptic transmission by multi-electrode array. Hippocampal slice placed over an 8×8 MEA. In CA1 (upper part — cell bodies indicated by white dashed line), stimulating electrode (upper blue triangle) was located under Schaffer collaterals, and evoked fEPSPs were monitored at proximal stratum radiatum and stratum pyramidale (upper white stars). Another stimulating electrode (green circle) was used as a second independent input in the CA1 region. In CA3 (lower part — cell bodies indicated by white dashed line) fEPSPs were recorded at the stratum radiatum (lower white star) by stimulating at the stratum lucidum (lower blue triangle). The white circle indicates the reference electrode. The white solid line indicates where the cut was made to prevent signals propagating from CA3 to CA1 regions. Waveforms of fEPSPs recorded by the different electrodes are superimposed.

in the CA1 region before LTP induction. Two stimulations with 50 ms inter-stimulus interval were applied 3 times with 10 s interval to obtain averaged values.

Confocal imaging of brain slices

After LTP recordings, 250 μm-thick slices were fixated in 4% paraformaldehyde for 30 min, washed with phosphate buffered saline (PBS) and embedded in 4% low gelling temperature agarose (Sigma, USA) dissolved in PBS (1 h at 4 °C). Embedded tissue was cut into 70 μm-thick sections on a vibratome. The middle sections were collected and incubated for 1.5 h in a blocking buffer (BB) containing 2% fetal calf serum, 2% bovine serum albumin, 0.2% gelatin, 0.3% Triton-X 100 and 5% goat serum dissolved in PBS. Sections were then incubated with primary anti-Aβ antibody 6E10 (1:500 in BB) at 4 °C overnight, and washed with PBS (3×5 min). Secondary antibody (goat anti-mouse-Alexa488, 1:500 in BB without goat serum) was applied for 3 h at room temperature, followed by washing with PBS (3×5 min). Slices without Aβ treatment were used as controls.

Finally, the sections were mounted on glass slides and coated with Moviol containing propidium iodide (1:250, Invitrogen, USA). Fluorescent images were obtained by a laser confocal Nikon A1R inverted microscope (Nikon, Japan) using a 10× plan Apo 0.45 dry objective.

Data acquisition and analysis

All data were collected at 10 kHz sampling frequency and 1100 amplifier gain. Triggered fEPSPs were recorded and processed by MC_Rack and MC_Data Tool software (Multi Channel Systems, Germany). All plotted data are shown as mean values ± the standard error of mean (mean ± S.E.M.). Data from transgenic and wild-type mice were compared by two-tailed student's *t*-test and two-way ANOVA with Tukey post hoc analysis. Values of $P<0.05$ were considered significant.

Results

Simultaneous recording of fEPSPs in CA3 and CA1

Electrical stimulation and recordings were simultaneously performed in the CA1 and CA3 regions of the same hippocampal slice. To avoid CA3 signals propagating to the CA1 region, slices were partially transected on the border between areas CA1 and CA3 (Fig. 1). Cut slices showed normal spontaneous and evoked responses as observed in uncut slices. fEPSPs from cut slices also followed typical signal patterns previously recorded from uncut slices by MEAs (Hofmann and Bading, 2006; Kopanitsa et al., 2006). In the CA1 region, fEPSPs were recorded by electrodes located maximum 600 μm away from the stimulating electrode which was located underneath the Schaffer collaterals. As shown in the waveforms of Fig. 1, CA1 proximal stratum radiatum displayed a large negative deflection, while a biphasic response was observed in the stratum pyramidale. In the CA3 region, stimulation of mossy fibers was performed through an electrode located in the stratum lucidum. The negative deflection of the extracellular potential signal recorded in the proximal radiatum was similar to that recorded in the CA1 area. Electrical stimulation of either Schaffer collaterals or mossy fibers in the same slice had no effect on simultaneous fEPSP recordings in the CA1 and CA3 regions.

Basal synaptic transmission

Basal synaptic transmission in each group of mice was assessed by measuring the amplitude of presynaptic fiber volleys (FV) and the slope of evoked fEPSP at different stimulus intensities (Fig. 2). I/O curves for CA3 region (Figs. 2D–F and Table 1) were generally similar in APP.V717I as well as biAT mice and not significantly different compared to wild-type mice. Only Tau.P301L mice showed a slight decrease in FV amplitude (Fig. 2E), however fEPSP slope and I/O relation were not affected (Figs. 2D and F). These results imply that there are no major differences in synaptic organization or basal transmission in CA3 of APP.V717I and biAT mice, on the other hand minimal effect was observed in Tau.P301L mice.

In the CA1 region, the I/O relation (Fig. 2C and Table 1) was slightly but significantly increased in biAT and Tau.P301L mice compared to wild-type and APP.V717I mice. In CA1 of Tau.P301L mice, a significant increase was apparent in both the fEPSP slope (Fig. 2A) and the FV amplitude (Fig. 2B) vs stimulus intensity. The effect is, therefore, pointing to increased FV enhancing transmitter release and EPSP in CA1 of Tau.P301L mice, and to a lesser extent in biAT mice. In biAT mice, the increase in the slope of the I/O curve was not apparent in the FV vs intensity amplitude (Figs. 2A and B). The data suggest a direct effect of protein tau on the synaptic efficacy of CA1 pyramidal neurons.

Short-term plasticity

We next investigated frequency-dependent facilitation (FF) and paired-pulse facilitation (PPF), two forms of short-term plasticity. FF is a pronounced property of the mossy fiber-CA3 synapse compared to any other type of synapses (Klausnitzer and Manahan-Vaughan, 2008; Nicoll and Schmitz, 2005; Salin et al., 1996). When the stimulus frequency was increased step-wise from 0.05 to 2 Hz, fEPSPs recorded in the CA3 region increased in amplitude and reached the maximal level within 40 s at each frequency (Fig. 3A). The magnitude of FF, expressed as the relative ratio of the maximal to the baseline amplitude, depended strongly on the stimulus frequency in the different genotypes. While there was no difference in FF between APP.V717I and wild-type mice, FF was dramatically enhanced at stimulation frequencies above 0.5 Hz in Tau.P301L mice. In biAT mice, on the other hand, FF was significantly reduced at stimulation frequencies above 1 Hz (Fig. 3B). Averaged FF values for the 3 transgenic strains and wild-type mice are summarized in Table 2.

PPF (inter-stimulus interval, 50 ms) was measured to analyze presynaptic function in CA1. We found no significant difference in PPF level between APP.V717I, Tau.P301L and wild-type mice. The PPF ratio amounted to 1.48 ± 0.05, 1.29 ± 0.05 and 1.43 ± 0.07 in APP.V717I, Tau.P301L and wild-type mice, respectively (Fig. 4). In biAT mice, PPF ratio was 1.27 ± 0.03 and slightly decreased relative to wild-type and APP.V717I mice. These results indicate that FF in CA3 and to a lesser extent PPF in CA1 are impaired in biAT mice, whereas Tau.P301L mice unexpectedly showed a pronouncedly enhanced FF in CA3, but normal PPF in CA1.

Long-term potentiation (LTP)

High frequency stimulation (HFS) induced LTP in CA1 and CA3 regions in all mouse strains (Fig. 5). CA1 LTP, quantified at 30 and 60 min following HFS, was significantly and to a similar extent reduced in all transgenic strains. At 60 min post-HFS, the magnitude of LTP was 306.3 ± 43.3% in wild-type animals as opposed to 169.7 ± 19.2%, 155.4 ± 6.1% and 171.1 ± 15.0% in APP.V717I, biAT and Tau.P301L, respectively relative to baseline (Figs. 5A and B). CA3 LTP, recorded at 30 and 60 min following HFS, did not significantly differ between wild-type, APP.V717I and Tau.P301L mice. At 60 min post-HFS, the LTP magnitude amounted to 221.7 ± 26.4%, 192.8 ± 26.9%, and 247.7 ± 44.4% in wild-type, APP.V717I and Tau.P301L respectively relative to baseline (Figs. 5C and D). In contrast, hippocampal slices from biAT mice showed a significantly lowered LTP at 60 min post-HFS, i.e. 150.5 ± 10.2% relative to baseline (Figs. 5C and D). The results indicate that whereas biAT mice and the parental amyloid and tau transgenic mouse models suffered severely impaired LTP in the CA1 region, only the combined amyloid and tau

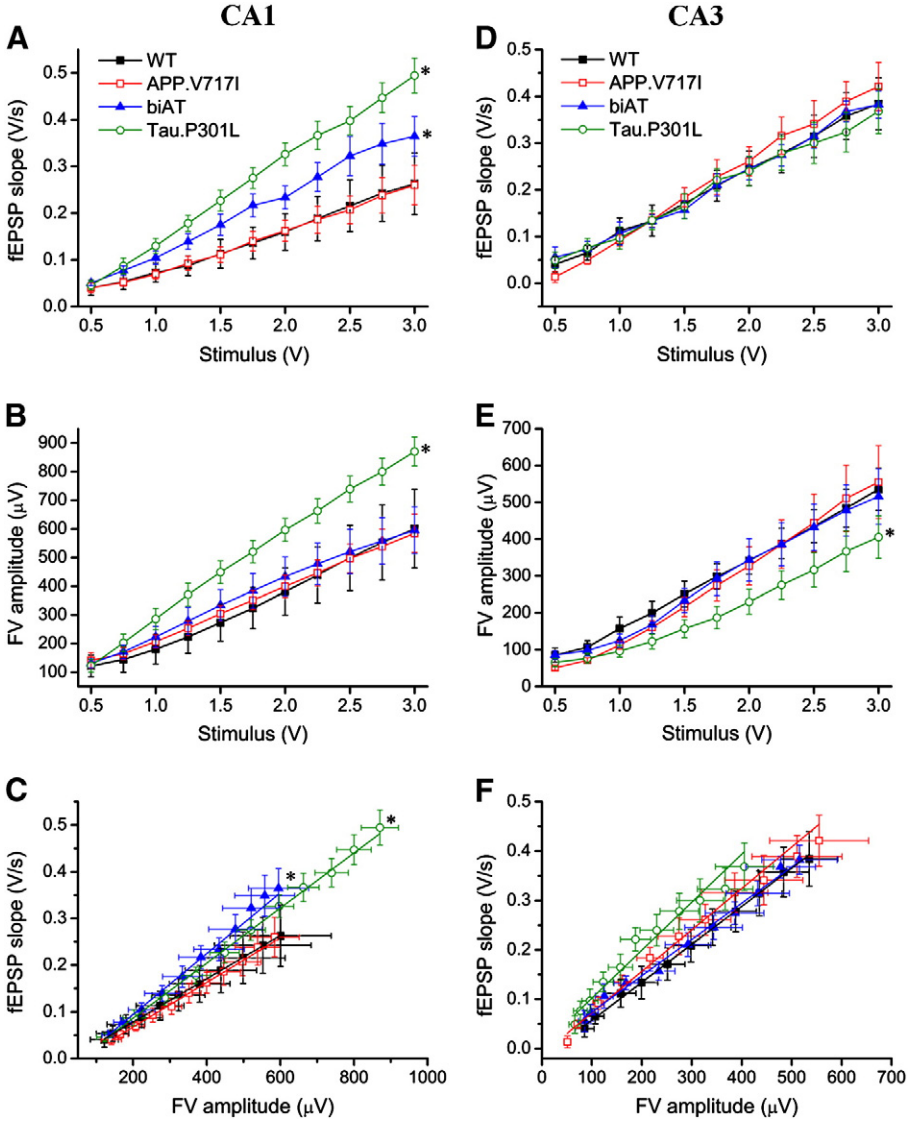

Fig. 2. Basal synaptic transmission in CA1 (A–C) and CA3 (D–F). Both fEPSP slope (A and D) and fiber volley (FV) amplitude (B and E) increased as a function of stimulus intensity. Input (FV amplitude) – output (fEPSP slope) relations (C and F) show that basal synaptic transmission is not affected in CA3 (F) but slightly increased in Tau.P301L and biAT mice in CA1. 2-way ANOVA with Tukey post hoc analysis measured differences between all groups and stimuli. (A) $P<0.0001$ Tau.P301L vs all other groups; biAT vs APP.V717I and WT. (B) $P<0.0001$ Tau.P301L vs all other groups. (C) $P<0.01$ Tau.P301L vs all other groups; biAT vs APP.V717I and WT. (E) $P<0.0001$ Tau.P301L vs all other groups. WT $n=8$ slices/4 mice, APP.V717I $n=6/4$, biAT $n=8/4$ and Tau.P301L $n=8/4$.

pathology in the biAT mice, caused a specific LTP impairment in the CA3 subfield of the hippocampus.

Consistent with the findings in APP.V717I mice, pre-treatment of hippocampal slices from wild-type mice with 1 μM Aβ42/40 (ratio 3:7) for 20 min suppressed LTP in CA1 but had no effect on CA3 LTP (Supplementary Fig. 1). This finding suggests that acute synaptotoxic effects of Aβ oligomers are CA1-specific.

Table 1
Linear fit slope values for Figs. 2C and F.

	CA1	CA3
WT	4.48E−4 ± 3.28E−5	7.71E−4 ± 6.66E−5
APP.V717I	5.03E−4 ± 7.87E−5	8.27E−4 ± 5.74E−5
biAT	7.17E−4 ± 6.75 E−5	8.38 E−4 ± 1.28E−4
Tau.P301L	6.01 E−4 ± 2.85E−5	9.42E−4 ± 1.26E−4

The values are indicated in V/s·μV (mean ± S.E.M).

Discussion

In this study we investigated the use of the MEA platform to simultaneously record synaptic activities in the CA1 and CA3 sub-regions in acute hippocampal slices from mouse brain. Principal features of synaptic transmission and plasticity were compared in three transgenic mouse models that are relevant to AD, relative to age-matched wild-type mice as controls (results are summarized in Table 3). Young adult (4–6 months of age) animals were evaluated to analyze early synaptic dysfunction before the onset or progression of the typical AD pathology of amyloid plaques and neurofibrillary tangles. In this time-window, the transgenic mice show already cognitive defects (Dewachter et al., 2000; Moechars et al., 1999; Terwel et al., 2005; 2008), making them models for MCI. MCI is increasingly recognized as the prodrome of Alzheimer's disease (review Allegri et al., 2008; and references therein) for which good models and markers are lacking. Moreover, tau transgenic mice have not been analyzed extensively in this respect. To our knowledge this is the first study that compares mice with amyloid and tau pathology separately and combined. In addition, all transgenes are expressed in

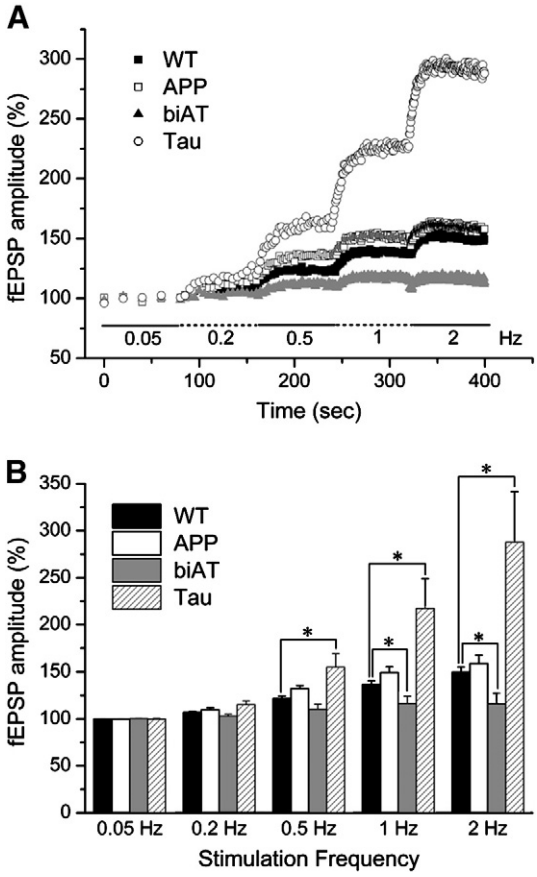

Fig. 3. Frequency facilitation (FF) at CA3 mossy fiber synapses. (A) Normalized fEPSP amplitude at different stimulus frequencies in wild-type (WT), APP.V717I (APP), biAT and Tau.P301L (Tau) mice. Averaged fEPSP amplitudes were normalized to that recorded at the basal frequency of 0.05 Hz. (B) Summarized data for frequency facilitation of fEPSPs at different stimulation frequencies. Compared to wild-type mice, frequency facilitation was significantly enhanced in Tau.P301L mice but significantly decreased in biAT mice. $^{*}P<0.05$. WT $n=10/4$, APP.V717I $n=7/4$, biAT $n=8/4$ and Tau.P301L $n=8/4$.

identical genetic background, making the data specific for the respective transgenes and relevant for the inflicted pathologies.

Recordings were primarily made in the CA1 and CA3 sub-regions because LTP in the CA1 region, like in the dentate gyrus, depends on activation of NMDA receptors, while potentiation at the mossy fibers (MF)-CA3 synapse is NMDA receptor-independent (Lynch, 2004; Nicoll and Schmitz, 2005). In all mouse strains, fEPSPs were successfully and simultaneously recorded in the CA1 and CA3 regions, when both regions were functionally separated by transsection as described in the Material and methods section. Basic features of fEPSPs and LTP in both regions were similar to those recorded in intact hippocampal slices by MEAs (Hofmann and Bading, 2006; Kopanitsa et al., 2006; Steidl et al., 2006) and by conventional extracellular glass

Table 2
Averaged FF responses.

	WT	APP.V717I	biAT	Tau.P301L
0.05 Hz	99.8 ± 0.1	99.8 ± 0.2	100.3 ± 0.3	99.9 ± 0.8
0.2 Hz	106.9 ± 0.9	109.6 ± 2.2	102.8 ± 2.1	115.1 ± 3.9
0.5 Hz	121.6 ± 2.9	132.2 ± 3.3	110.3 ± 5.3	154.8 ± 14.4
1 Hz	136.7 ± 3.9	149.5 ± 5.4	116.4 ± 7.8	217.3 ± 31.6
2 Hz	149.8 ± 5.0	158.5 ± 8.9	115.9 ± 11.4	287.7 ± 53.8

The averaged FF responses at each stimulation frequency (0.2, 0.5, 1 and 2 Hz) were normalized to the value at 0.05 Hz. Values are mean ± S.E.M (%). WT $n=10/4$, APP.V717I $n=7/4$, biAT $n=8/4$ and Tau.P301L $n=8/4$.

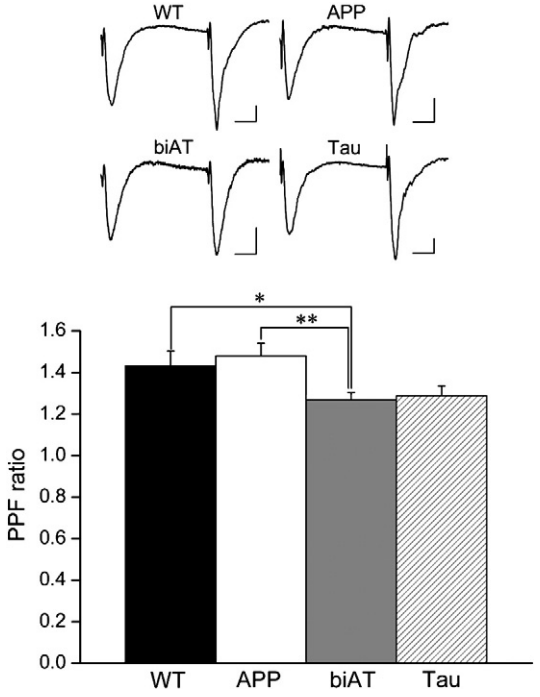

Fig. 4. Paired pulse facilitation (PPF) in CA1. PPF was measured in CA1 stratum radiatum. Sample traces show fEPSPs evoked by paired-pulse stimulation at 50 ms inter-stimulus interval in wild-type (WT), APP.V717I (APP), biAT and Tau.P301L (Tau) mice (scale bar Y: 0.1 mV, X: 10 ms). The bar graph summarizes averaged PPF ratio values. APP.V717I and Tau.P301L mice did not differ from wild-type mice. Only biAT mice exhibited significantly reduced PPF compared to wild-type and APP.V717I mice. $^{*}P<0.05$, $^{**}P<0.01$. WT $n=11/4$, APP.V717I $n=10/4$, biAT $n=11/4$ and Tau.P301L $n=12/4$.

electrodes (Sarvey et al., 1989; Zhang et al., 2009). We conclude that the experimental data validate the MEA approach suitable and relevant for simultaneous electrophysiological recordings in mouse hippocampal sub-regions.

We observed a significant reduction of NMDA-dependent LTP in the CA1 region in young APP.V717I and Tau.P301L mice. In addition, CA1 LTP was reduced to a similar degree in age-matched double-transgenic biAT mice. These data are in line with our previous data in young APP.V717I mice by conventional single electrode analysis (Moechars et al., 1999) but extend them to Tau.P301L and to the biAT model. Impaired CA1 LTP, with presynaptic function (PPF) unaffected or slightly increased was observed in other APP models (Giacchino et al., 2000; Larson et al., 1999). In most APP models basal synaptic transmission was normal (Chapman et al., 1999; Larson et al., 1999; Liu et al., 2008; Moechars et al., 1999) or slightly reduced (Fitzjohn et al., 2001). The LTP deficit in CA1 in APP.V717I mice is thought to be caused by soluble Aβ oligomers that disrupt postsynaptic NMDA receptor function (Dewachter et al., 2009; Li et al., 2009; Yamin, 2009). On the other hand, LTP in CA3 is presynaptic and NMDA receptor-independent (Nicoll and Schmitz, 2005), which would explain why LTP was not affected in CA3 of APP.V717I mice. Furthermore, the finding that Aβ oligomers diminished CA1 LTP but had no effect on CA3 LTP in wild-type mice supports the idea that synaptic dysfunction in CA1 of young APP.V717I mice is related to increased levels of soluble Aβ peptides in the brain, which lead to mild memory deficits at this age (Moechars et al., 1999).

Impaired LTP in CA1 was also observed in Tau.P301L mice, concomitant with increased synaptic excitability. Moreover, PPF after LTP induction was significantly decreased in CA1 of wild-type mice, indicating an increase in release probability after LTP induction, but not affected in Tau.P301L mice (data not shown). These findings were unexpected, because most previous studies in single or double mutant tau models did not observe altered synaptic transmission in

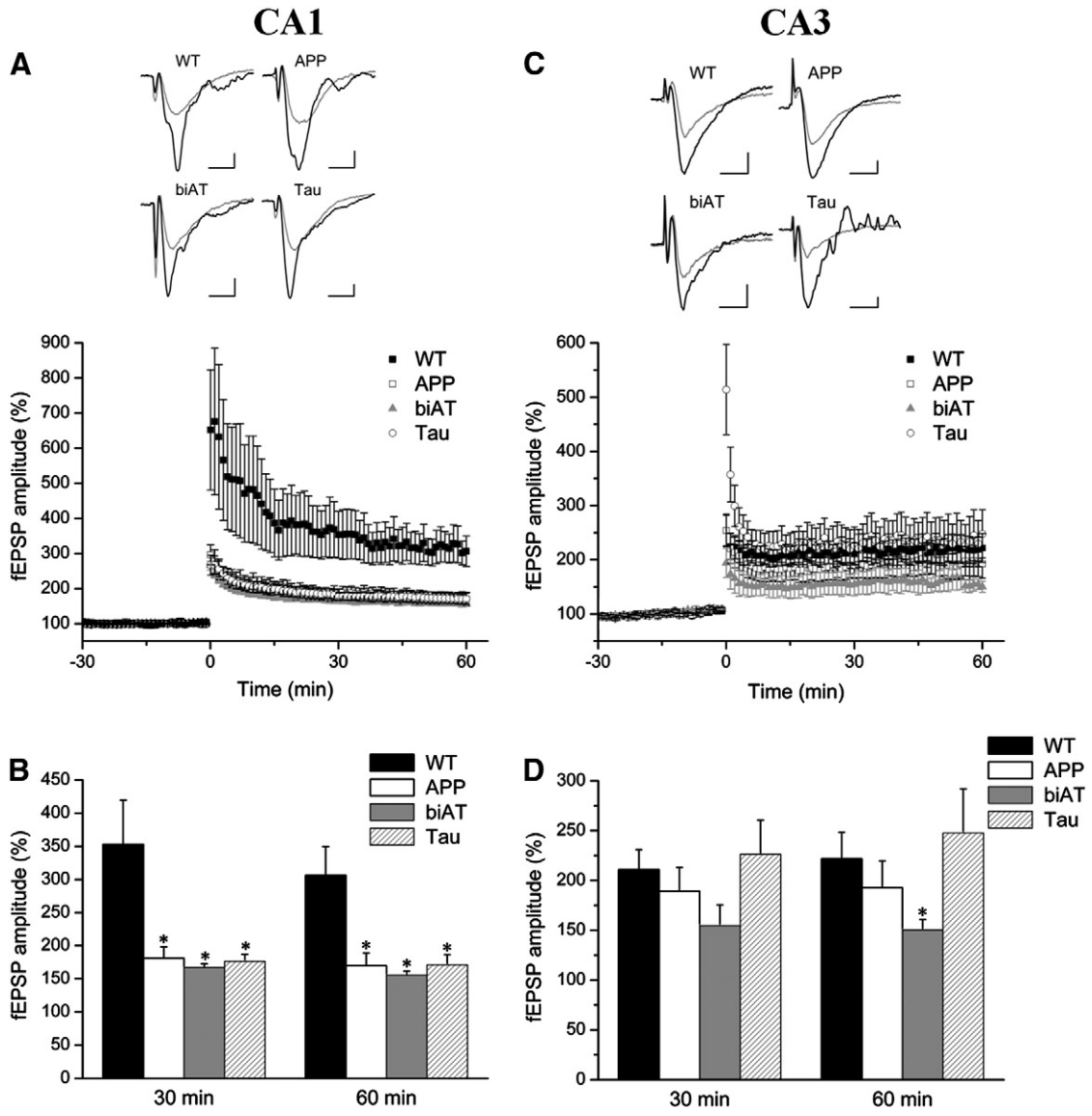

Fig. 5. Long-term potentiation (LTP) in CA1 (A–B) and CA3 (C–D). After 30 min of base line recordings, 2 sets of HFS (100 Hz) were applied to induce LTP in CA1 and CA3. (A and C) Sample traces above show fEPSPs recorded before (grey) and 30 min after HFS (black, scale bar Y: 0.1 mV, X: 5 ms). Normalized fEPSPs values plotted as a function of time for wild-type (WT) and transgenic animals. (B and D) Pooled data for wild-type and the different transgenic animals showing LTP levels at 30 min and 60 min after HFS. *$P<0.05$. WT $n=7/4$, APP.V717I $n=14/7$, biAT $n=8/4$ and Tau.P301L $n=8/4$.

CA1 at this age (Schindowski et al., 2006, for review see Denk and Wade-Martins, 2009). We previously reported improved cognitive performance and enhanced LTP in the dentate gyrus of young (8–10 weeks) Tau.P301L mice (Boekhoorn et al., 2006). Only few studies reported pronounced learning and memory deficits in double mutant (K257T/P301S) and mutant (P301L) human tau mice (Hoover et al., 2010; Rosenmann et al., 2008). These early synaptic effects of tau are proposed to be closely related to the presence of abnormally phosphorylated tau as soluble aggregates, that we have termed Tau-P*

Table 3
Overview of synaptic activity changes in three AD transgenic mice.

	CA1			CA3		
	Basal	STP	LTP	Basal	STP	LTP
APP.V717I	–	–	↓↓	–	–	–
biAT	↑	↓	↓↓	–	↓	↓
Tau.P301L	↑↑	–	↓↓	–	↑↑	–

The levels of synaptic activity in each genotype were compared to those of wild-type mice. – No change, ↑/↓ moderate increase/decrease, ↑↑/↓↓ large increase/decrease.

(Boekhoorn et al., 2006; Jaworski et al., 2009, 2010; Terwel et al., 2005). Furthermore, the LTP deficit in CA1 might imply that tau-mediated pathology affects mainly postsynaptic elements, in line with a dendritic function of tau e.g. hyperphosphorylated tau mislocalization to dendrites leading to a decreased number of functional AMPA and NMDA receptors (Hoover et al., 2010; Ittner et al., 2010; Ittner and Goetz, 2011). Interestingly, our current findings that LTP in CA1 is impaired while LTP in CA3 is normal in Tau.P301L mice nicely, corroborate recent work showing that intracerebral injection of viral vector to express Tau.P301L in hippocampus, leads to degeneration of CA1 pyramidal neurons but spares CA3 pyramidal cells (Jaworski et al., 2009). However, a presynaptic effect of tau cannot be excluded since we observed reduced neurotransmitter release probability in CA1 of Tau.P301L mice. In addition, previous studies highlighted the role of presynaptic mechanisms in the expression of LTP at CA1 synapses (Lauri et al., 2007; Roggenhofer et al., 2010). Therefore further investigations are needed to explore the role of tau in presynaptic plasticity.

Meanwhile short-term (FF) and long-term (LTP) synaptic plasticity in CA3 were not depressed in Tau.P301L mice. Both FF and LTP at

MF-CA3 synapses are thought to rely mainly on presynaptic mechanisms involving Ca^{2+} homeostasis at mossy fiber nerve terminals, tightly controlled by membrane potentials and mitochondrial Ca^{2+} handling (Billups and Forsythe, 2002; Nicoll and Schmitz, 2005). Rocher et al. (2010) recently reported that cortical pyramidal cells of Tau.P310L mice display depolarized resting membrane potentials (±8 mV) and associated increase in action potential firing rates, possibly reflecting ATP depletion and mitochondrial dysfunction (David et al., 2005). Thus, subtle changes in nerve terminal potential and/or mitochondrial function, inflicted by axonal protein tau, might underlie the increase in synaptic facilitation and potentiation in CA3 hippocampal neurons of Tau.P301L mice (Ittner et al., 2009; Mandelkow et al., 2004). Finally, the increased synaptic activity in CA3 might correlate with previous data showing improved memory performance and exploratory behavior in 2–6 month-old Tau.P301L mice (Boekhoorn et al., 2006; Pennanen et al., 2006).

The observed reduced LTP in CA1 of young biAT transgenic mice agrees with findings in a similar model, i.e. the 3xTg model that, however, expresses also a mutant presenilin-1 (Oddo et al., 2003), which can disturb observations of the effects of amyloid and protein tau (Zhang et al., 2009). Our observations extend the impact because we compare biAT mice to their parental APP.V717I and Tau.P301L mice, which is not possible with the 3xTg model. The LTP impairment in CA1 of biAT mice was similar to that in the parental or single transgenic animals indicating that the LTP deficit in CA1 was (i) affected similarly by amyloid and by protein tau and (ii) already reached a maximum level in the parental mice. Importantly, however, in contrast to the parental mice, biAT mice displayed LTP as well as FF deficits in the CA3 regions. Previously, we observed that biAT mice exhibited aggravated tauopathy and amyloid deposition with cognitive and behavioral defects from young age (Terwel et al., 2008). Mutant tau therefore not only triggers LTP defects itself, but also exacerbates synaptic deficits caused by amyloid oligomers. The data help to explain the defects in primary tauopathies, as well as the essential contribution of protein tau to Aβ peptide toxicity (Ittner and Goetz, 2011; Roberson et al., 2007, 2011). Therefore our findings underline the role of protein tau in, and its contribution to MCI and eventually to its conversion to AD. The molecular and cellular defects inflicted by protein tau in axons and presynaptic compartments need to be defined in detail.

In conclusion, our data validated MEAs as rapid and effective tools for analyzing phenotypically different transgenic mouse models. We demonstrated that the dual electrophysiological recording method is adequate and reliable to monitor early and region-specific defects inflicted by amyloid and tau pathology in AD transgenic mouse models, separately and combined. Our results reveal that APP.V717I×Tau.P301L bigenic mice suffer severe deficits in synaptic plasticity in both the CA3 and CA1 regions whereas single transgenic animals only display deficits in synaptic plasticity in the CA1 region.

Supplementary materials related to this article can be found online at doi:10.1016/j.nbd.2011.07.006.

Disclosure statement

The authors declare that there are no actual or potential conflicts of interest.

Acknowledgments

We thank Dr. Frank Hofmann, Hanne Verachtert and Erik De Prins for helpful technical assistance. We also thank Dr. Dries Braeken for scientific discussion. LEGTEGG gratefully acknowledges support by Fonds Wetenschappelijk Onderzoek-Vlaanderen (FWO-Vlaanderen), Instituut voor Wetenschap en Techniek (IWT), EEC-Framework Programs, KULeuven-Research Fund (BOF), and KULeuven-Research & Development. This work was partially supported by a Methusalem grant of KULeuven and the Flemish Government (Prof. B.D.S.), and a MEMOSAD (F2-2007-200611) of the European Union.

References

Allegri, R.F., Glaser, F.B., Taragano, F.E., Buschke, H., 2008. Mild cognitive impairment: believe it or not? Int. Rev. Psychiatry 20, 357–363.
Arnold, F.J.L., Hofmann, F., Bengtson, C.P., Wittmann, M., Vanhoutte, P., Bading, H., 2005. Microelectrode array recordings of cultured hippocampal networks reveal a simple model for transcription and protein synthesis-dependent plasticity. J. Physiol. 564, 3–19.
Billups, B., Forsythe, I.D., 2002. Presynaptic mitochondrial calcium sequestration influences transmission at mammalian central synapses. J. Neurosci. 22, 5840–5847.
Boekhoorn, K., Terwel, D., Biemans, B., Borghgraef, P., Wiegert, O., Ramakers, G.J.A., de Vos, K., Krugers, H., Tomiyama, T., Mori, H., Joels, M., Van Leuven, F., Lucassen, P.J., 2006. Improved long-term potentiation and memory in young tau-P301L transgenic mice before onset of hyperphosphorylation and tauopathy. J. Neurosci. 26, 3514–3523.
Chapman, P.F., White, G.L., Jones, M.W., Cooper-Blacketer, D., Marshall, V.J., Irizarry, M., Younkin, L., Good, M.A., Bliss, T.V.P., Hyman, B.T., Younkin, S.G., Hsiao, K.K., 1999. Impaired synaptic plasticity and learning in aged amyloid precursor protein transgenic mice. Nat. Neurosci. 2, 271–276.
David, D.C., Hauptmann, S., Scherping, I., Schuessel, K., Keil, U., Rizzu, P., Ravid, R., Droese, S., Brandt, U., Mueller, W.E., Eckert, A., Goetz, J., 2005. Proteomic and functional analyses reveal a mitochondrial dysfunction in P301L tau transgenic mice. J. Biol. Chem. 280, 23802–23814.
Denk, F., Wade-Martins, R., 2009. Knock-out and transgenic mouse models of tauopathies. Neurobiol. Aging 30, 1–13.
Dewachter, I., van Dorpe, J., Spittaels, K., Tesseur, I., Ven Den Haute, C., Moechars, D., Van Leuven, F., 2000. Modeling Alzheimer's disease in transgenic mice: effect of age and of Presenilin1 on amyloid biochemistry and pathology in APP/London mice. Exp. Gerontol. 35, 831–841.
Dewachter, I., Filipkowski, R.K., Priller, C., Ris, L., Neyton, J., Croes, S., Terwel, D., Gysemans, M., Devijver, H., Borghgraef, P., Godaux, E., Kaczmarek, L., Herms, J., Van Leuven, F., 2009. Deregulation of NMDA-receptor function and down-stream signaling in APP[V717I] transgenic mice. Neurobiol. Aging 30, 241–256.
Dutschmann, M., Menuet, C., Stettner, G.M., Gestreau, C., Borghgraef, P., Devijver, H., Gielis, L., Hilaire, G., Van Leuven, F., 2010. Upper airway dysfunction of Tau-P301L mice correlates with tauopathy in midbrain and ponto-medullary brainstem nuclei. J. Neurosci. 30, 1810–1821.
Fitzjohn, S.M., Morton, R.A., Kuenzi, F., Rosahl, T.W., Shearman, M., Lewis, H., Smith, D., Reynolds, D.S., Davies, C.H., Collingridge, G.L., Seabrook, G.R., 2001. Age-related impairment of synaptic transmission but normal long-term potentiation in transgenic mice that overexpress the human APP695SWE mutant form of amyloid precursor protein. J. Neurosci. 21, 4691–4698.
Giacchino, J., Criado, J.R., Games, D., Henriksen, S., 2000. In vivo synaptic transmission in young and aged amyloid precursor protein transgenic mice. Brain Res. 876, 185–190.
Goetz, J., Ittner, L.M., 2008. Animal models of Alzheimer's disease and frontotemporal dementia. Nat. Rev. Neurosci. 9, 532–544.
Hill, A.J., Jones, N.A., Williams, C.M., Stephens, G.J., Whalley, B.J., 2010. Development of multi-electrode array screening for anticonvulsants in acute rat brain slices. J. Neurosci. Methods 185, 246–256.
Hofmann, F., Bading, H., 2006. Long term recordings with microelectrode arrays: studies of transcription-dependent neuronal plasticity and axonal regeneration. J. Physiol. Paris 99, 125–132.
Hoover, B.R., Reed, M.N., Su, J., Penrod, R.D., Kotilinek, L.A., Grant, M.K., Pitstick, R., Carlson, G.A., Lanier, L.M., Yuan, L.L., Ashe, K.H., Liao, D., 2010. Tau mislocalization to dendritic spines mediates synaptic dysfunction independently of neurodegeneration. Neuron 68, 1067–1081.
Hsia, A.Y., Masliah, E., McConlogue, L., Yu, G.Q., Tatsuno, G., Hu, K., Kholodenko, D., Malenka, R.C., Nicoll, R.A., Mucke, L., 1999. Plaque-independent disruption of neural circuits in Alzheimer's disease mouse models. Proc. Natl. Acad. Sci. 96, 3228–3233.
Ittner, L.M., Goetz, J., 2011. Amyloid-β and tau — a toxic pas de deux in Alzheimer's disease. Nat. Rev. Neurosci. 12, 67–72.
Ittner, L.M., Ke, Y.D., Goetz, J., 2009. Phosphorylated tau interacts with c-Jun N-terminal kinase-interacting protein 1 (JIP1) in Alzheimer disease. J. Biol. Chem. 284, 20909–20916.
Ittner, L.M., Ke, Y.D., Delerue, F., Bi, M., Gladbach, A., van Eersel, J., Wolfing, H., Chieng, B.C., Christie, M.J., Napier, I.A., Eckert, A., Staufenbiel, M., Hardeman, E., Goetz, J., 2010. Dendritic function of tau mediates amyloid-β toxicity in Alzheimer's disease mouse models. Cell 142, 387–397.
Jaworski, T., Dewachter, I., Lechat, B., Croes, S., Termont, A., Demedts, D., Borghgraef, P., Devijver, H., Filipkowski, R.K., Kaczmarek, L., Kugler, S., Van Leuven, F., 2009. AAV-tau mediates pyramidal neurodegeneration by cell-cycle re-entry without neurofibrillary tangle formation in wild-type mice. PloS One 4, e7280.
Jaworski, T., Dewachter, I., Seymour, C.M., Borghgraef, P., Devijver, H., Kügler, S., Van Leuven, F., 2010. Alzheimer's disease: old problem, new views from transgenic and viral models. Biochim. Biophys. Acta. 1802, 808–818.
Klausnitzer, J., Manahan-Vaughan, D., 2008. Frequency facilitation at mossy fiber-CA3 synapses of freely behaving rats is regulated by adenosine A1 receptors. J. Neurosci. 28, 4836–4840.

Kopanitsa, M.V., Afinowi, O., Grant, S.G.N., 2006. Recording long-term potentiation of synaptic transmission by three-dimensional multi-electrode arrays. BMC Neurosci. 7, 61.

Kuperstein, I., Broersen, K., Benilova, I., Rozenski, J., Jonckheere, W., Debulpaep, M., Vandersteen, A., Segers-Nolten, I., Van Der Werf, K., Subramaniam, V., Braeken, D., Callewaert, G., Bartic, C., D'Hooge, R., Martins, I.C., Rousseau, F., Schymkowitz, J., De Strooper, B., 2010. Neurotoxicity of Alzheimer's disease Aβ peptides is induced by small changes in the $A\beta_{42}$ to $A\beta_{40}$ ratio. EMBO J. 29, 3408–3420.

Larson, J., Lynch, G., Games, D., Seubert, P., 1999. Alterations in synaptic transmission and long-term potentiation in hippocampal slices from young and aged PDAPP mice. Brain Res. 840, 23–35.

Lauri, S.E., Palmer, M., Segerstrale, M., Vesikansa, A., Taira, T., Collingridge, G.L., 2007. Presynaptic mechanisms involved in the expression of STP and LTP at CA1 synapses in the hippocampus. Neuropharmacol. 52, 1–11.

Lewis, J., Dickson, D.W., Lin, W.L., Chisholm, L., Corral, A., Jones, G., Yen, S.H., Sahara, N., Skipper, L., Yager, D., Eckman, C., Hardy, J., Hutton, M., McGowan, E., 2001. Enhanced neurofibrillary degeneration in transgenic mice expressing mutant tau and APP. Science 293, 1487–1491.

Li, X.N., Zhou, W., Zeng, S.Q., Liu, M., Luo, Q.M., 2007. Long-term recording on multi-electrode array reveals degraded inhibitory connection in neuronal network development. Biosens. Bioelectron. 22, 1538–1543.

Li, S.M., Hong, S.Y., Shepardson, N.E., Walsh, D.M., Shankar, G.M., Selkoe, D., 2009. Soluble oligomers of amyloid beta protein facilitate hippocampal long-term depression by disrupting neuronal glutamate uptake. Neuron 62, 788–801.

Liu, L., Orozco, I.J., Planel, E., Wen, Y., Bretteville, A., Krishnamurthy, P., Wang, L., Herman, M., Figueroa, H., Yu, W.H., Arancio, O., Duff, K., 2008. A transgenic rat that develops Alzheimer's disease-like amyloid pathology, deficits in synaptic plasticity and cognitive impairment. Neurobiol. Dis. 31, 46–57.

Lynch, M.A., 2004. Long-term potentiation and memory. Physiol. Rev. 84, 87–136.

Mandelkow, E.M., Thies, E., Trinczek, B., Biernat, J., Mandelkow, E., 2004. MARK/PAR1 kinase is a regulator of microtubule-dependent transport in axons. J. Cell Biol. 167, 99–110.

Moechars, D., Dewachter, I., Lorent, K., Reverse, D., Baekelandt, V., Naidu, A., Tesseur, I., Spittaels, K., Van Den Haute, C., Checler, F., Godaux, E., Cordell, B., Van Leuven, F., 1999. Early phenotypic changes in transgenic mice that overexpress different mutants of amyloid precursor protein in brain. J. Biol. Chem. 274, 6483–6492.

Nicoll, R.A., Schmitz, D., 2005. Synaptic plasticity at hippocampal mossy fibre synapses. Nat. Rev. Neurosci. 6, 863–876.

Oddo, S., Caccamo, A., Shepherd, J.D., Murphy, M.P., Golde, T.E., Kayed, R., Metherate, R., Mattson, M.P., Akbari, Y., LaFerla, F.M., 2003. Triple-transgenic model of Alzheimer's disease with plaques and tangles: intracellular A beta and synaptic dysfunction. Neuron 39, 409–421.

Oka, H., Shimono, K., Ogawa, R., Sugihara, H., Taketani, M., 1999. A new planar multielectrode array for extracellular recording: Application to hippocampal acute slice. J. Neurosci. Methods 93, 61–67.

Pennanen, L., Wolfer, D.P., Nitsch, R.M., Goetz, J., 2006. Impaired spatial reference memory and increased exploratory behavior in P301L tau transgenic mice. Genes Brain Behav. 5, 369–379.

Roberson, E.D., Scearce-Levie, K., Palop, J.J., Yan, F., Cheng, I.H., Wu, T., Gerstein, H., Yu, G.Q., Mucke, L., 2007. Reducing endogenous tau ameliorates amyloid β-induced deficits in an Alzheimer's disease mouse model. Science 316, 750–754.

Roberson, E.D., Halabisky, B., Yoo, J.W., Yao, J., Chin, J., Yan, F., Wu, T., Hamto, P., Devidze, N., Yu, G.Q., Palop, J.J., Noebels, J.L., Mucke, L., 2011. Amyloid-β/Fyn-induced synaptic, network, and cognitive impairments depend on tau levels in multiple mouse models of Alzheimer's disease. J. Neurosci. 31, 700–711.

Rocher, A.B., Crimins, J.L., Amatrudo, J.M., Kinson, M.S., Todd-Brown, M.A., Lewis, J., Luebke, J.I., 2010. Structural and functional changes in tau mutant mice neurons are not linked to the presence of NFTs. Exp. Neurol. 223, 385–393.

Roggenhofer, E., Fidzinski, P., Bartsch, J., Kurz, F., Shor, O., Behr, J., 2010. Activation of dopamine D1/D5 receptors facilitates the induction of presynaptic long-term potentiation at hippocampal output synapses. Eur. J. Neurosci. 32, 598–605.

Rosenmann, H., Grigoriadis, N., Eldar-Levy, H., Avital, A., Rozenstein, L., Touloumi, O., Behar, L., Ben-Hur, T., Avraham, Y., Berry, E., Segal, M., Ginzburg, I., Abramsky, O., 2008. A novel transgenic mouse expressing double mutant tau driven by its natural promoter exhibits tauopathy characteristics. Exp. Neurol. 212, 71–84.

Saganich, M.J., Schroeder, B.E., Galvan, V., Bredesen, D.E., Koo, E.H., Heinemann, S.F., 2006. Deficits in synaptic transmission and learning in amyloid precursor protein (APP) transgenic mice require C-terminal cleavage of APP. J. Neurosci. 26, 13428–13436.

Salin, P.A., Scanziani, M., Malenka, R.C., Nicoll, R.A., 1996. Distinct short-term plasticity at two excitatory synapses in the hippocampus. Proc. Natl. Acad. Sci. U.S.A. 93, 13304–13309.

Sarvey, J.M., Burgard, E.C., Decker, G., 1989. Long-term potentiation studies in the hippocampal slice. J. Neurosci. Methods 28, 109–124.

Schindowski, K., Bretteville, A., Leroy, K., Begard, S., Brion, J.P., Hamdane, M., Buee, L., 2006. Alzheimer's disease-like tau neuropathology leads to memory deficits and loss of functional synapses in a novel mutated tau transgenic mouse without any motor deficits. Am. J. Pathol. 169, 599–616.

Steidl, E.M., Neueu, E., Bertrand, D., Buisson, B., 2006. The adult rat hippocampal slice revisited with multi-electrode arrays. Brain Res. 1096, 70–84.

Terwel, D., Lasrado, R., Snauwaert, J., Vandeweert, E., Van Haesendonck, C., Borghgraef, P., Van Leuven, F., 2005. Changed conformation of mutant tau-P301L underlies the moribund tauopathy, absent in progressive, nonlethal axonopathy of tau-4R/2N transgenic mice. J. Biol. Chem. 280, 3963–3973.

Terwel, D., Muyllaert, D., Dewachter, I., Borghgraef, P., Croes, S., Devijver, H., Van Leuven, F., 2008. Amyloid activates GSK-3 beta to aggravate neuronal tauopathy in bigenic mice. Am. J. Pathol. 172, 786–798.

Yamin, G., 2009. NMDA receptor-dependent signaling pathways that underlie amyloid beta-protein disruption of LTP in the hippocampus. J. Neurosci. Res. 87, 1729–1736.

Yeckel, M.F., Kapur, A., Johnston, D., 1999. Multiple forms of LTP in hippocampal CA3 neurons use a common postsynaptic mechanism. Nat. Neurosci. 2, 625–633.

Zhang, C., Wu, B., Beglopoulos, V., Wines-Samuelson, M., Zhang, D.W., Dragatsis, I., Sudhof, T.C., Shen, J., 2009. Presenilins are essential for regulating neurotransmitter release. Nature 460, 632–636.